Journal of Solid State Chemistry **151,** 181–189 (2000)
doi:10.1006/jssc.2000.8633, available online at http://www.idealibrary.com on IDEAL®

Crystal Structure of $Pb_5Bi_{18}P_4O_{42}$: A Fluorite-Related Superstructure

Sophie Giraud,*,† Jean-Pierre Wignacourt,* Steve Swinnea,† Hugo Steinfink,† and Richard Harlow‡

*Laboratoire de Cristallochimie et Physicochimie du Solide, URA CNRS 452, ENSCL, BP 108, 59652 Villeneuve d'Ascq Cedex, France,
†Texas Materials Institute and Department of Chemical Engineering, University of Texas, Austin, Texas 78712; and ‡The DuPont Company CRD, E228/316d, Wilmington, Delaware 19880-0228

Received October 20, 1999; in revised form January 11, 2000; accepted January 20, 2000

Single crystals of a new oxyphosphate of bismuth and lead, $Pb_5Bi_{18}P_4O_{42}$, were studied using short-wavelength synchrotron X-ray radiation. The compound is monoclinic, *I*2/*m*, $a = 11.885(2)$ Å, $b = 11.540(2)$ Å, $c = 15.636(3)$ Å, $\beta = 90.23(3)^\circ$, $Z = 2$. The crystal is twinned by pseudo-merohedry. The structure refinement converged to $R = 0.0366$. There are five crystallographically independent Bi atoms. The oxygen coordination polyhedron around Bi(1) is a slightly distorted cube with Bi–O bonds varying from 2.381(11) to 2.662(10) Å. The other four Bi atoms are in a severely distorted oxygen environment with bond lengths varying from 2.102(5) to 3.16(2) Å. A greater variation of the oxygen coordination polyhedra exists around the three crystallographically independent Pb atoms changing from a somewhat elongated cube to a monocapped pentagonal bipyramid; bond distances vary from 2.13(2) to 3.38(2) Å. Of 20 crystallographically independent oxygen ions 11 are disordered. The structure consists of two Bi–O layers parallel to (101). They are interconnected perpendicular to [010] by layers consisting of Pb and PO_4. The two crystallographically independent PO_4 moieties are disordered. This compound displays a δ-Bi_2O_3 fluorite superstructure. The locations of the nonbonded lone-pair electrons were calculated and vary from 0 to 1.1 Å. These displacements from the cation nucleus are indicative of the extent of *s*–*p* hybridization, where zero displacement represents the spherical nonbonded $6s^2$ orbital. The extent of hybridization is a function of the distortion of the oxygen coordination polyhedron around the cation.

Key Words: **$Pb_5Bi_{18}P_4O_{42}$; structure; disorder; $Pb_5Bi_{18}P_4O_{42}$; lone-pair electrons and coordination polyhedra, influence of.**

INTRODUCTION

Bi_2O_3 exhibits four different structure types (1–3). The high-temperature fluorite type δ-Bi_2O_3 is well known as one of the best anionic conductors due to oxygen vacancies in the structure (4). The discovery that $Bi_4V_2O_{11}$ was a good oxide ion conductor (5) spawned intensive research on this and related phases (6). An extensive review by Boivin and Mairesse discusses recent developments in fast oxide ion conductors (7). Many studies of bismuth-based oxides have been carried out and numerous compounds with high bismuth content have been reported as having a fluorite superstructure (8–13). The pseudo-ternary systems PbO–Bi_2O_3–M_2O_5 (M = P, V, As) have been extensively investigated (14–20) and recently we discovered new compounds with the formula $Pb_5Bi_{18}M_4O_{42}$ (M = P, V, As). They are related to a fluorite type superstructure. This paper reports the structure of the new phase $Pb_5Bi_{18}P_4O_{42}$.

EXPERIMENTAL

Bi_2O_3 (Strem 99.9%) and PbO (Alfa 99.97%) were preheated overnight at 600°C to remove any carbonate. They were mixed with $(NH_4)_2HPO_4$ (Strem 99 + %) in stoichiometric ratios to obtain phases $Pb_{4+x}Bi_{19-x}P_4O_y$ ($x = 0, 1$). These stoichiometric compositions were chosen because the exploration of the tie line $PbBiPO_5$–Bi_2O_3 (20) led to the discovery of a new phase near those stoichiometries. The mixtures containing the phosphate were slowly heated at 300°C to decompose $(NH_4)_2HPO_4$.

Initially the samples were examined by X-ray diffraction with a Guinier–de Wolf camera and Cu$K\alpha$ radiation. Subsequently, powder patterns were recorded with Cu$K\alpha$ radiation using an automated D5000 Siemens diffractometer equipped with a diffracted beam graphite monochromator. Differential thermal analysis (DTA) was performed on a Linseis L62 instrument. Density measurements were done with an automated Micrometritics Accupyc 1330 gas picnometer equipped with a 1-cm^3 cell. The possibility of phase transitions was checked with a high-temperature X-ray diffraction (HTXRD) Guinier–Lenné camera at a heating rate of 20°C min^{-1}.

The melting point of $Pb_5Bi_{18}P_4O_{42}$ is 930°C and single crystals were obtained by melting the powder in a gold crucible. The powder was heated in air to 970°C for 3 h, slowly cooled at a rate of 1.2°C/h to 850°C, and then furnace cooled to room temperature. The crystals are light yellow needles. Single crystals were selected under a polarizing microscope and Weissenberg photographs were obtained.

0022-4596/00 $35.00

The reciprocal lattice photographs indicated an apparent I-centered orthorhombic cell. The data for the structure determination were recorded with synchrotron radiation, $\lambda = 0.1602$ Å, as part of a DuPont program to study the general effect of absorption on crystal structure determinations. The data were collected using an MAR-CCD detector on beamline 5BMD at the Advanced Photon Source, Argonne National Laboratory. A total of 64 frames were collected: 300 sec per frame, 3 deg oscillation, $\lambda = 0.1602$ Å, at a crystal-to-detector distance of 200 mm. The program DENZO (21) was used to analyze the frames yielding a C-centered monoclinic unit cell, $a = 19.602$ Å, $b = 11.540$ Å, $c = 11.885$ Å, $\beta = 127.09°$. The intensity data were then extracted and merged, $R(F) = 0.046$ and $R(F^2) = 0.039$. No absorption correction was made since $\mu_1 = 1.67$ mm^{-1}. The unit cell was reoriented to yield the nonstandard monoclinic I-centered unit cell, $a = 11.885(2)$ Å, $b = 11.540(2)$ Å, $c = 15.636(3)$ Å, $\beta = 90.23(3)°$, to emphasize the nearly orthogonal β angle. The crystal data and refinement are shown in Table 1. The structure was solved using the direct method and refined by full-matrix least squares (22, 23). Pb, Bi, and P atoms were refined anisotropically, while O atoms were refined isotropically. The least-squares refinement was based on 3498 unique reflections $I > 2\sigma(I)$ and converged to $R = 0.0366$.

TABLE 1
Crystal Data and Refinement for $Pb_5Bi_{18}P_4O_{42}$

Crystallographic Data	
Formula	$Pb_5Bi_{18}P_4O_{42}$
Color	Light yellow
Crystal system	Monoclinic
Space group	$I2/m$
a (Å)	11.885(2)
b (Å)	11.540(2)
c (Å)	15.636(3)
β (°)	90.23(3)
Volume (Å^3)	2144.5(7)
Z	2
Formula weight (g/mol)	5593.47
Measured/calculated density (g/cm^3)	8.62/8.68
Intensity Collection	
Radiation (Å)	0.1602
μ_1 (mm^{-1})	1.67
Temperature (°C)	298
θ range	0.93–8.08°
Data collected	$-16 \le h \le 20$, $0 \le k \le 20$, $-15 \le l \le 27$
No. of reflections measured	6258
No. of uniqaue reflections $I > 2\sigma(I)$	3498
$R(F^2)_{int}$	0.039
Refinement	
Parameters varied	142
Refinement method	Least squares on F^2
Twin function	100, 0 −10, 00 −1
Twin fraction	0.26
$R(F)$ obs/all	0.0366/0.0744
$R_w(F^2)$ obs/all	0.0787/0.1568
$w = 1/(\sigma^2(F_o^2) + (XP)^2 + 0.00P)$ with $P = (F_o^2 + 2F_c^2)/3$	$X = 0.045$
GOF obs/all	0.682/0.559
Max., min, $\Delta\rho$, e Å^{-3}	7.868, −7.971

TABLE 2
Powder X-Ray Diffraction Diagram of $Pb_5Bi_{18}P_4O_{42}$

h	k	l	d_{obs} (Å)	d_{cal} (Å)	I (%)	h	k	l	d_{obs} (Å)	d_{cal} (Å)	I (%)
1	0	1	9.491	9.489	8	1	4	−3	2.482	2.482	<1
0	1	1	9.324	9.330	1	2	4	2	2.473	2.473	<1
1	1	0	8.296	8.320	1	2	0	−6	2.403	2.404	<1
0	0	2	7.872	7.859	<1	0	2	6	2.387	2.387	<1
0	2	0	5.787	5.797	3	4	3	−1	2.339	2.338	1
1	1	−2	5.738	5.723	2	4	3	1	2.332	2.333	<1
1	1	2	5.708	5.704	1	0	4	4	2.317	2.317	<1
2	1	1	5.028	5.024	7	3	2	−5	2.276	2.275	<1
1	2	1	4.945	4.947	<1	3	3	−4	2.271	2.270	<1
1	0	3	4.794	4.790	1	2	3	−5	2.261	2.261	1
0	1	3	4.771	4.775	6	2	3	5	2.255	2.255	2
3	0	−1	3.863	3.865	<1	5	1	−2	2.244	2.246	<1
3	1	0	3.768	3.766	3	2	2	6	2.212	2.213	<1
2	1	3	3.721	3.721	<1	0	1	7	2.204	2.205	<1
1	2	−3	3.702	3.700	<1	4	2	4	2.195	2.196	<1
1	1	−4	3.556	3.558	2	5	2	−1	2.190	2.189	<1
1	1	4	3.550	3.549	1	5	2	1	2.186	2.186	<1
3	1	−2	3.408	3.403	<1	2	4	−4	2.174	2.175	1
1	3	−2	3.333	3.333	4	2	4	4	2.171	2.171	<1
1	3	2	3.330	3.329	1	3	1	−6	2.156	2.155	1
2	0	−4	3.289	3.291	1	3	1	6	2.146	2.146	<1
3	2	−1	3.216	3.216	1	2	5	−1	2.142	2.142	1
3	0	−3	3.178	3.178	76	3	4	3	2.137	2.137	1
3	0	3	3.162	3.163	100	0	5	3	2.120	2.120	<1
0	3	3	3.109	3.110	94	2	1	−7	2.072	2.072	<1
1	0	−5	3.042	3.044	4	2	1	7	2.067	2.065	<1
1	0	5	3.036	3.037	2	1	2	−7	2.064	2.064	2
0	4	0	2.898	2.898	1	5	1	−4	2.016	2.015	<1
2	2	−4	2.863	2.862	<1	5	1	4	2.006	2.006	2
2	2	4	2.849	2.852	1	6	0	0	1.991	1.991	16
4	1	1	2.843	2.842	1	0	4	6	1.944	1.944	1
4	0	−2	2.796	2.797	8	0	6	0	1.933	1.932	15
4	0	2	2.788	2.787	8	3	3	−6	1.908	1.908	17
3	3	0	2.773	2.773	45	3	3	6	1.901	1.901	19
0	0	6	2.619	2.620	22	4	3	−5	1.893	1.893	3
4	1	−3	2.536	2.537	<1	4	3	5	1.886	1.886	2
4	1	3	2.528	2.527	<1						

Note. Lattice parameters: $a = 11.946(3)$ Å, $b = 11.592(3)$ Å, $c = 15.719(3)$ Å, $\beta = 90.29(1)°$; Cu $K\alpha$.

RESULTS

All observed lines of the powder pattern of $Pb_5Bi_{18}P_4O_{42}$ were indexed. The unit cell parameters were refined by least squares. The indexed powder pattern and lattice parameters are shown in Table 2. There is a significant difference between the single-crystal and powder diffraction cell parameters. The synchrotron wavelength was determined using

the Au K absorption edge and is accurate. However, the crystal-to-detector distance is less precise and a small error in that distance will greatly impact the cell parameters. We attempted to quantify the Pb/Bi ratio using standardless X-ray energy dispersive techniques (EDX) but the results were not definitive. The Pb/Bi ratios varied from 0.25 to 0.29. The synthesis of a stoichiometric mixture to yield $Pb_6Bi_{17}P_4O_y$ seemed to have the same powder X-ray diffraction pattern as the $Pb_5Bi_{18}P_4O_{42}$ phase but $Pb_4Bi_{19}P_4O_7$ showed weak lines of a second phase. We believe that $Pb_5Bi_{18}P_4O_{42}$ exhibits a slight range of solid solubility and that may also account for the differences in the lattice parameters obtained from the single crystal and the powder.

The measured density of the phosphate compound, $\rho = 8.62\ g/cm^3$, yields two formula weights of $Pb_5Bi_{18}P_4O_{42}$ per unit cell. No indications of a phase transition were observed on DTA and HTXRD. When the data were merged on the basis of an orthorhombic symmetry R_{int} was unacceptably high while $R(F^2)_{int}$ is 0.039 for a monoclinic system. The space group $I2$ was chosen initially and 13 heavy atoms resulting from the direct method and subsequent Fourier maps were introduced, yielding $R = 0.165$. Including parameters of two P atoms obtained from a difference electron density map dropped R to 0.14. A center of symmetry was now identified and the refinement was continued in the centrosymmetric group $I2/m$. At this stage R was 0.15. The oxygen atomic positions were obtained from successive Fourier difference maps. Fourteen oxygen atoms were found. The displacement parameters were refined anisotropically for Pb, Bi, and P, and isotropically for oxygen atoms. The refinement converged to $R = 0.064$ but some of the oxygen atoms required for the PO_4 groups were still missing.

Monoclinic cells with $\beta \cong 90°C$ often twin by a rotation of 180° about the a axis, (100, 0 −10, 00 −1), displaying a pseudo-orthorhombic cell. This twinning function was introduced in the refinement, dropping the R value to 0.0377. The fraction of the twin is 26%. At this point some oxygen atoms were still missing from the PO_4 groups. The examination of difference Fourier maps revealed some additional peaks of low density at reasonable positions from phosphorus to form tetrahedra and they were assigned to oxygen atoms. It became evident that multiple tetrahedra were centered on the two crystallographically independent phosphorus atoms. The very low electron density peaks are due to the partial site occupancies (sof) by oxygen. P(1) is bonded to O(9), O(10), 2 O(11), 2 O(16), and O(17). The sof for O(9) is 1. The sum of the sof's of the other oxygen atoms was restrained to form two PO_4 tetrahedra, Fig. 1. P(2) is bonded to O(12), 2 O(13), O(14), O(15), 2 O(18), 2 O(19), and O(20). The coordinates of O(14) and O(20) were fixed because they were ill-behaved during least-squares refinements. The bond distance P(2)–O(15) was restrained to a value greater than 1.4 Å. Without such a restraint least-squares refinements yielded values of about 1.35 Å. Restraints were also applied to the sof's of oxygen atoms around P(2) so that the total number of oxygen atoms yielded three PO_4 moieties, Fig. 1. Isotropic displacement parameters of oxygen were obtained by least-squares refinements. The last cycle of refinement yielded $R = 0.0366$. Table 3 lists the final atomic parameters, Table 4 the anisotropic displacement parameters, and Table 5 the interatomic bond lengths and angles, the bond valences, and their sums (24).

LONE-PAIR LOCALIZATION

The interplay among lone-pair electrons, stereochemistry, and crystal structure has long been of interest to crystallographers and solid-state chemists (25–27). Verbaere *et al.* (28) developed the theory enabling the calculation for

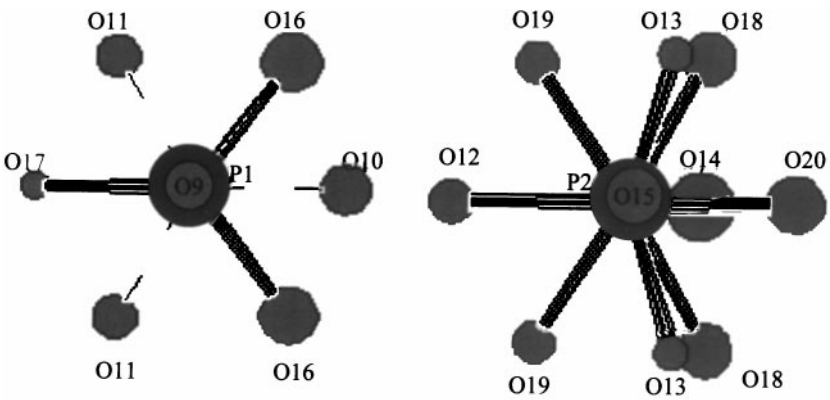

FIG. 1. Oxygen environment around P(1) and P(2). All oxygen atoms are shown to illustrate the disorder. The dashed and full bonds show the two tetrahedra around P(1). O(9) is above P(1) and O(15) above P(2).

TABLE 3
Atomic Coordinates and Equivalent Displacement Parameters, Å², for $Pb_5Bi_{18}P_4O_{42}$

Atom	Occupancy	x	y	z	U_{eq}[a]
Bi(1)	1	0.5	0.17676(4)	0.5	0.0380(2)
Bi(2)	1	0.16189(4)	0.16729(3)	0.17434(3)	0.0219(1)
Bi(3)	1	0.65596(4)	0.33241(3)	0.32187(3)	0.0208(1)
Bi(4)	1	0.68436(3)	0.33988(2	−0.00402(4)	0.0198(1)
Bi(5)	1	−0.00413(5)	0.33894(3)	0.34941(2)	0.0191(1)
Pb(1)	1	0	0	0	0.0323(2)
Pb(2)	1	0.66636(8)	0	0.33797(6)	0.0380(2)
Pb(3)	1	0.34985(8)	0	0.32457(6)	0.0373(2)
P(1)	1	0.4984(5)	0.5	−0.1572(2)	0.0163(6)
P(2)	1	−0.2981(3)	0	0.0026(4)	0.0190(7)
O(1)	1	0.765(1)	0.5	0.015(1)	0.020(2)
O(2)	1	0.503(2)	0	0.396(1)	0.036(2)
O(3)	1	0.183(1)	0.318(1)	0.097(1)	0.026(2)
O(4)	1	0.811(1)	0.304(1)	0.090(1)	0.027(2)
O(5)	1	0.012(2)	0.5	0.287(1)	0.026(2)
O(6)	1	0.003(2)	0.169(1)	0.101(1)	0.069(3)
O(7)	1	0.635(1)	0.187(1)	0.240(1)	0.041(2)
O(8)	1	0.133(2)	0.295(1)	0.270(1)	0.064(3)
O(9)	1	0.608(2)	0.5	−0.110(2)	0.073(6)
O(10)	0.77(2)	0.518(3)	0.5	0.752(2)	0.067(6)
O11)	0.77(2)	0.430(2)	0.605(1)	0.864(1)	0.051(3)
O(12)	0.84(2)	0.635(2)	0	0.086(2)	0.046(4)
O(13)	0.54(2)	0.679(2)	0.891(2)	0.951(2)	0.027(3)
O(14)	0.54(2)	0.821	0	0.031	0.103(15)
O(15)	0.46(2)	0.616(5)	0	0.939(4)	0.083(14)
O(16)	0.24(2)	0.995(8)	0.102(5)	0.718(5)	0.089(17)
O(17)	0.24(2)	0.606(5)	0.5	0.098(4)	0.021(8)
O(18)	0.29(2)	0.261(4)	0.393(3)	0.484(4)	0.065(11)
O(19)	0.16(2)	0.177(7)	0.397(5)	0.552(5)	0.044(15)
O(20)	0.16(2)	0.809	0	0.952	0.081(38)

[a] U_{eq} is defined as $\frac{1}{3}$ of the trace of the diagonalized U_{ij} tensor.

localizing the lone-pair electrons in a crystal structure. It is based on the local electric field calculation in the whole crystal using Ewald's method (29) and was recently successfully applied to several materials (26, 30, 31). It was incorporated in the computer program HYBRIDE (31). The required mean ionicity for the three cations was calculated for $Pb_5Bi_{18}P_4O_{42}$ from the electronegativity differences using the formula

$$M\text{–O} = 1 - \exp[-(X_O - X_M)^2/4].$$

These values provided the oxidation state $+1.22$ for Pb^{2+}, 1.7 for Bi^{3+}, and $+2.0$ for P^{5+}. The oxygen atoms were given the balancing charge -1.06 to ensure electroneutrality within the lattice. The positions of the lone-pair electrons of Pb and Bi are shown in Table 6. These distances reflect the displacement of the electron density of the s–p hybridized orbital from the nucleus. A zero distance means that the spherical $6s^2$ orbital is centered on the nucleus as expected and no hybridization has occurred. With increasing displacements from the nucleus the s–p hybridization increases and it is directly correlated with the distortion of the oxygen polyhedron around the cation.

TABLE 4
Anisotropic Displacement Parameters for Bi, Pb, and P, Å²

Atom	U_{11}	U_{22}	U_{33}	U_{23}	U_{13}	U_{12}
Bi(1)	0.0481(5)	0.0211(2)	0.0447(4)	0	−0.0061(5)	0
Bi(2)	0.0252(2)	0.0156(2)	0.0248(2)	0.0037(2)	−0.0077(2)	0.0003(2)
Bi(3)	0.0214(2)	0.0170(2)	0.0238(2)	0.0046(2)	0.0035(2)	0.0016(2)
Bi(4)	0.0179(2)	0.0173(1)	0.0243(2)	−0.0010(2)	−0.0008(2)	−0.0033(2)
Bi(5)	0.0187(2)	0.0218(1)	0.0167(2)	0.0044(2)	−0.0008(2)	−0.0005(2)
Pb(1)	0.0605(7)	0.0148(2)	0.0217(3)	0	0.0098(6)	0
Pb(2)	0.0353(4)	0.0380(3)	0.0408(5)	0	0.0150(4)	0
Pb(3)	0.0323(4)	0.0445(3)	0.0349(4)	0	−0.0158(4)	0
P(1)	0.019(2)	0.0134(8)	0.017(2)	0	−0.002(2)	0
P(2)	0.016(2)	0.0140(8)	0.027(2)	0	0.001(2)	0

Note. The anisotropic displacement exponent takes the form $-2\pi^2[h^2a^{x2}U_{11} + \cdots + 2hka^xb^xU_{12}]$.

DISCUSSION

The Pb and Bi atoms display a number of different coordination polyhedra. Bi(1) is bonded to eight oxygen atoms that have full site occupancies at the distances shown in Table 5. They form a slightly distorted cube around Bi(1). Fig. 2A. The calculated position of the electron lone pair, 0.21 Å, is very close to the nucleus. We ascribe this proximity to the nucleus as due to the electrostatic repulsion by the nearly regular array of oxygen anions around Bi(1). The valence bond sum of 2.32 may be indicative of a mixed Bi/Pb site occupancy. Bi(2) is coordinated by the fully occupied sites of O(3), O(6), and 2 O(8), to one of the disordered O(10) sof 0.76, or O(16) sof 0.24, and to one of the disordered O(13) sof 0.54, O(18) sof 0.29, or O(20) sof 0.16. The sof's were restrained in the least-squares refinements to add to unity for each set of disordered oxygen ions. The coordination polyhedron using only O(16) and O(18) is shown in Fig. 2A. Five anions form a nearly rectangular pyramid with O(3) occupying the apex. The lone-pair electrons push the sixth atom, O(16), away from what otherwise would be a position to complete an octahedron. The lone pair is 0.41 Å from the nucleus. The use of other combinations of partially occupied oxygen sites creates similar polyhedra. This is also the case for the other Bi coordination polyhedra. The coordination polyhedron around Bi(3) is very similar to that of Bi(2), Fig. 2A. The lone-pair electrons are 0.54 Å from the nucleus. Bi(4) is coordinated to O(1), O(3), O(4), and O(9) whose sites are fully occupied and to one O(11) sof 0.76, or O(17) sof 0.12, and to one of the three ions O(13) sof 0.54, O(18) sof 0.29, or O(19) sof 0.16, Fig. 2A. The sof's in each case were restrained to sum to unity. The lone pair is 1.1 Å from the nucleus indicating the largest extent of s–p

TABLE 5
(A) Bond Lengths (Å) and (B) Selected Angles (deg) for $Pb_5Bi_{18}P_4O_{42}$

(A) Bond Lengths

Bi(1)–O(6)#1	2.381(11)	0.46	Bi(4)–O(1)	2.102(5)	0.98	Pb(2)–O(2)	2.15(2)	0.90
Bi(1)–O(6)	2.381(11)	0.46	Bi(4)–O(4)	2.142(9)	0.88	Pb(2)–O(1)#4	2.436(10)	0.42
Bi(1)–O(2)	2.609(8)	0.25	Bi(4)–O(3)#11	2.157(10)	0.86	Pb(2)–O(4)#4	2.542(8)	0.31
Bi(1)–O(2)#3	2.609(8)	0.25	Bi(4)–O(17)	2.62(4)	0.06[a]	Pb(2)–O(4)#24	2.542(8)	0.31
Bi(1)–O(3)#1	2.639(9)	0.23	Bi(4)–O(9)	2.64(2)	0.23	Pb(2)–O(7)#22	2.677(10)	0.22
Bi(1)–O(3)#2	2.639(9)	0.23	Bi(4)–O(11)#8	2.66(2)	0.17[a]	Pb(2)–O(7)	2.677(10)	0.22
Bi(1)–O(4)#4	2.662(10)	0.22	Bi(4)–O(13)#12	2.750(14)	0.09[a]	Pb(2)–O(5)#1	2.874(12)	0.13
Bi(1)–O(4)#5	2.662(10)	0.22	Bi(4)–O(18)#13	2.85(3)	0.04[a]	Pb(2)–O(17)#4	2.88(5)	0.03[a]
Valence bond sum		2.32	Bi(4)–O(19)#13	2.87(6)	0.02[a]	Pb(2)–O(11)#25	3.38(2)	
Bi(2)–O(8)	2.122(13)	0.93	Valence bond sum		3.31	Pb(2)–O(11)#13	3.38(2)	
Bi(2)–O(3)	2.137(8)	0.89	Bi(5)–O(7)#1	2.107(11)	0.97	Valence bond sum		2.54
Bi(2)–O(6)	2.20(2)	0.75	Bi(5)–O(5)	2.112(5)	0.95	Pb(3)–O(2)	2.13(2)	0.95
Bi(2)–O(8)#1	2.626(15)	0.24	Bi(5)–O(8)	2.117(15)	0.94	Pb(3)–O(5)#1	2.394(13)	0.47
Bi(2)–O(16)#7	2.63(8)	0.06[a]	Bi(5)–O(12)#1	2.630(15)	0.19[a]	Pb(3)–O(3)#1	2.474(8)	0.38
Bi(2)–O(18)#1	2.74(5)	0.05[a]	Bi(5)–O(19)#15	2.65(8)	0.04[a]	Pb(3)–O(3)#23	2.474(8)	0.38
Bi(2)–O(20)#3	2.7820(6)	0.03[a]	Bi(5)–O(15)#16	2.72(4)	0.08[a]	Pb(3)–O(8)#23	2.800(12)	0.16
Bi(2)–O(13)#8	2.81(2)	0.08[a]	Bi(5)–O(13)#9	2.76(2)	0.09[a]	Pb(3)–O(8)#1	2.800(12)	0.16
Bi(2)–O(10)#9	2.85(2)	0.10[a]	Bi(5)–O(11)#9	2.816(13)	0.11[a]	Pb(3)–O(9)#6	3.05(2)	0.08
Valence bond sum		3.13	Bi(5)–O(16)#7	2.93(5)	0.02[a]	Pb(3)–O(1)#6	3.147(10)	0.06
Bi(3)–O(4)#4	2.127(8)	0.91	Valence bond sum		3.39	Valence bond sum		2.64
Bi(3)–O(7)	2.128(10)	0.91	Pb(1)–O(14)#17	2.1849(5)	0.45[a]	P(1)–O(9)	1.50(2)	
Bi(3)–O(6)#1	2.25(2)	0.66	Pb(1)–O(14)#18	2.1849(5)	0.45[a]	P(1)–O(10)#26	1.44(2)	
Bi(3)–O(16)#10	2.62(8)	0.24	Pb(1)–O(20)#19	2.3935(6)	0.08[a]	P(1)–O(11)#12	1.499(14)	
Bi(3)–O(7)#4	2.672(12)	0.21	Pb(1)–O(20)#3	2.3935(6)	0.08[a]	P(1)–O(11)#26	1.499(14)	
Bi(3)–O(19)#7	2.89(7)	0.02[a]	Pb(1)–O(6)	2.510(11)	0.34			
Bi(3)–O(14)#4	3.0172(6)	0.04[a]	Pb(1)–O(6)#20	2.510(11)	0.34	P(1)–O(9)	1.50(2)	
Bi(3)–O(10)#8	3.05(2)	0.06[a]	Pb(1)–O(6)#21	2.510(11)	0.34	P(1)–O(16)#27	1.51(6)	
Bi(3)–O(11)#8	3.16(2)	0.05[a]	Pb(1)–O(6)#22	2.510(11)	0.34	P(1)–O(16)#5	1.51(6)	
Valence bond sum		3.10	Pb(1)–O(18)#1	3.11(5)	0.02[a]	P(1)–O(17)#28	1.55(5)	
			Pb(1)–O(18)#23	3.11(5)	0.02[a]			
			Pb(1)–O(18)#9	3.11(5)	0.02[a]			
			Pb(1)–O(18)#10	3.11(5)	0.02[a]			
			Valence bond sum		2.50			
P(2)–O(12)#18	1.53(2)		P(2)–O(15)#19	1.43(5)		P(2)–O(12)#18	1.53(2)	
P(2)–O(15)#19	1.43(5)		P(2)–O(19)#10	1.46(6)		P(2)–O(14)#18	1.481(4)	
P(2)–O(18)#10	1.45(4)		P(2)–O(19)#9	1.46(6)		P(2)–O(13)#29	1.521(15)	
P(2)–O(18)#9	1.45(4)		P(2)–O(20)#19	1.500(5)		P(2)–O(13)#30	1.521(15)	

(B) Selected Angles

O(6)#1–Bi(1)–O(6)#2	83.2(6)	O(1)–Bi(4)–O(4)	75.8(3)	O(6)–Pb(1)–O(6)#20	180.0
O(6)#1–Bi(1)–O(2)	99.8(3)	O(1)–Bi(4)–O(3)#11	82.2(3)	O(6)–Pb(1)–O(6)#21	78.1(5)
O(6)#2–Bi(1)–O(2)	176.6(4)	O(4)–Bi(4)–O(3)#11	85.4(3)	O(6)#20–Pb(1)–O(6)#21	101.9(5)
O(6)#2–Bi(1)–O(2)#3	99.8(3)	O(1)–Bi(4)–O(9)	68.2(4)		
O(2)–Bi(1)–O(2)#3	77.2(4)	O(4)–Bi(4)–O(9)	143.6(4)	O(2)–Pb(2)–O(1)#4	84.4(4)
O(6)#1–Bi(1)–O(3)#1	65.9(5)	O(3)#11–Bi(4)–O(9)	85.1(5)	O(2)–Pb(2)–O(4)#4	84.6(3)
O(6)#2–Bi(1)–O(3)#1	111.8(5)			O(1)#4–Pb(2)–O(4)#4	63.1(2)
O(2)–Bi(1)–O(3)#1	71.1(4)	O(7)#1–Bi(5)–O(5)	83.5(4)	O(4)#4–Pb(2)–O(4)#24	125.8(4)
O(2)#3–Bi(1)–O(3)#1	111.3(4)	O(7)#1–Bi(5)–O(8)	98.4(4)	O(4)#24–Pb(2)–O(7)#22	63.3(3)
O(6)#1–Bi(1)–O(3)#2	111.8(5)	O(5)–Bi(5)–O(8)	82.4(5)	O(2)–Pb(2)–O(7)	96.9(3)
O(3)#1–Bi(1)–O(3)#2	177.2(3)			O(1)#4–Pb(2)–O(7)	126.0(2)
O(6)#1–Bi(1)–O(4)#4	66.3(5)	O(10)#26–P(1)–O(9)	110.0(15)	O(4)#24–Pb(2)–O(7)	170.8(3)
O(6)#2–Bi(1)–O(4)#4	106.0(5)	O(10)#26–P(1)–O(11)#12	107.8(9)	O(7)#22–Pb(2)–O(7)	107.5(4)
O(2)–Bi(1)–O(4)#4	74.0(4)	O(9)–P(1)–O(11)#12	111.4(7)	O(2)–Pb(2)–O(5)#1	67.6(4)
O(2)#3–Bi(1)–O(4)#4	114.0(4)	O(11)#12–P(1)–O(11)#26	108.4(12)	O(1)#4–Pb(2)–O(5)#1	152.0(4)
O(3)#1–Bi(1)–O(4)#4	113.0(2)			O(4)#4–Pb(2)–O(5)#1	112.1(2)
O(3)#2–Bi(1)–O(4)#4	66.8(2)	O(9)–P(1)–O(16)#4	105.0(33)	O(7)–Pb(2)–O(5)#1	60.7(3)
O(4)#4–Bi(1)–O(4)#5	170.4(3)	O(16)#27–P(1)–O(16)#4	102.5(46)		
		O(9)–P(1)–O(17)#28	113.8(18)	O(2)–Pb(3)–O(5)#1	78.2(5)
O(8)–Bi(2)–O(3)	81.9(4)	O(16)#4–P(1)–O(17)#28	114.6(33)	O(2)–Pb(3)–O(3)#1	82.7(3)
O(8)–Bi(2)–O(6)	102.6(5)			O(5)#1–Pb(3)–O(3)#1	118.2(2)

TABLE 5—*Continued*

(B) Selected Angles

O(3)–Bi(2)–O(6)	78.3(4)	O(15)#19–P(2)–O(18)#10	101.9(22)	O(3)#1–Pb(3)–O(3)#23	116.6(4)
O(8)–Bi(2)–O(8)#1	78.6(6)	O(18)#10–P(2)–O(18)#9	116.7(35)	O(3)#1–Pb(3)–O(8)#23	175.0(4)
O(3)–Bi(2)–O(8)#1	86.8(4)	O(15)#19–P(2)–O(12)#18	102.9(22)	O(2)–Pb(3)–O(8)#1	102.2(4)
O(6)–Bi(2)–O(8)#1	164.6(5)	O(18)#10–P(2)–O(12)#18	115.1(19)	O(5)#1–Pb(3)–O(8)#1	64.3(3)
				O(3)#1–Pb(3)–O(8)#1	63.6(3)
O(4)#4–Bi(3)–O(7)	80.2(4)	O(15)#19–P(2)–O(19)#10	103.1(31)	O(8)#23–Pb(3)–O(8)#1	115.7(6)
O(4)#4–Bi(3)–O(6)#1	78.4(4)	O(19)#10–P(2)–O(18)#9	110.0(54)	O(2)–Pb(3)–O(9)#6	128.8(6)
O(7)–Bi(3)–O(6)#1	102.9(4)	O(15)#19–P(2)–O(20)#19	103.5(22)	O(5)#1–Pb(3)–O(9)#6	153.1(5)
O(4)#4–Bi(3)–O(7)#4	90.2(3)	O(19)#10–P(2)–O(20)#19	117.3(29)	O(3)#1–Pb(3)–O(9)#6	71.5(3)
O(7)–Bi(3)–O(7)#4	79.7(4)			O(8)#1–Pb(3)–O(9)#6	104.3(4)
O(6)#1–Bi(3)–O(7)#4	167.6(4)	O(14)#18–P(2)–O(13)#29	109.0(7)	O(2)–Pb(3)–O(1)#6	77.3(4)
		O(13)#29–P(2)–O(13)#30	112.3(12)	O(5)#1–Pb(3)–O(1)#6	155.4(4)
		O(14)#18–P(2)–O(12)#18	104.2(8)	O(3)#1–Pb(3)–O(1)#6	58.3(2)
		O(13)#29–P(2)–O(12)#18	111.0(8)	O(8)#1–Pb(3)–O(1)#6	121.5(3)
				O(9)#6–Pb(3)–O(1)#6	51.5(5)

Note. Symmetry transformations used to generate equivalent atoms: # 1 $-x+\frac{1}{2}, -y+\frac{1}{2}, -z+\frac{1}{2}$; #2 $x+\frac{1}{2}, -y+\frac{1}{2}, z+\frac{1}{2}$; #3, $-x+1, -y, -z+1$; #4 $x+\frac{3}{2}, -y+\frac{1}{2}, -z+\frac{1}{2}$; #5 $x-\frac{1}{2}, -y+\frac{1}{2}, z+\frac{1}{2}$; #6 $x-\frac{1}{2}, y-\frac{1}{2}, z+\frac{1}{2}$; #7 $-x+1, y, -z+1$; #8 $-x+1, -y+1, -z+1$; #9 $x-\frac{1}{2}, y-\frac{1}{2}, z-\frac{1}{2}$; #10 $x-\frac{1}{2}, -y+\frac{1}{2}, z-\frac{1}{2}$; #11 $-x+1, y, -z$; #12 $x, -y+1, z-1$; #13 $x+\frac{1}{2}, -y+\frac{1}{2}, z-\frac{1}{2}$; #14 $x, -y+1, z$; #15 $-x, y, -z+1$; #16 $x-\frac{1}{2}, y+\frac{1}{2}, z-\frac{1}{2}$; #17 $-x+1, -y, -z$; #18 $x-1, y, z$; #19 $x-1, y, z-1$; #20 $-x, -y, -z$; #21 $+x, y, -z$; #22 $x, -y, z$; #23 $-x+\frac{1}{2}, y-\frac{1}{2}, -z\frac{1}{2}$; #24 $-x+\frac{3}{2}, y-\frac{1}{2}, -z+\frac{1}{2}$; #25 $x+\frac{1}{2}, y-\frac{1}{2}, z-\frac{1}{2}$; #26 $x, y, z-1$; #27 $-x+\frac{3}{2}, y+\frac{1}{2}, -z+\frac{1}{2}$; #28 $-x+1, -y+1, -z$; #29 $x-1, y-1, z-1$; #30 $x-1, -y+1, z-1$; #31 $x+\frac{1}{2}, y+\frac{1}{2}, z-\frac{1}{2}$; #32 $x+1, y, z$; #33 $-x+\frac{1}{2}, y+\frac{1}{2}, -z+\frac{1}{2}$; #34 $-x+\frac{3}{2}, y+\frac{1}{2}, -z+\frac{3}{2}$; #35 $-x+\frac{3}{2}, -y+\frac{1}{2}, -z+\frac{3}{2}$; #36 $x, y, z+1$; #37 $x+\frac{1}{2}, y+\frac{1}{2}, z+\frac{1}{2}$; #38 $x, y-1, z-1$; #39 $x, y+1, z$; #40 $x+1, y+1, z+1$; #44 $x, y+1, z+1$; #42 $x, -y+2, z$; #43 $x+\frac{1}{2}, -y+\frac{3}{2}, z+\frac{1}{2}$; #44 $x, -y+1, z1$; #45 $x+1, y, z+1$; #46 $x, y-1, z$; #47 $x+\frac{1}{2}, y-\frac{1}{2}, z+\frac{1}{2}$; #48 $-x+\frac{3}{2}, y-\frac{1}{2}, -z+\frac{3}{2}$; #49 $x-\frac{1}{2}, y+\frac{1}{2}, z+\frac{1}{2}$; #50 $x-\frac{1}{2}, -y+\frac{3}{2}, z-\frac{1}{2}$. [a]The valence bond values for disordered atoms were calculated by multiplying v.b. by sof.

hybridization. Bi(5) is coordinated to the fully occupied sites by O(5), O(7), O(8); to one of the disordered O(11) sof 0.76, or O(16) sof 0.24; to one of O(12) sof 0.42, or O(19) sof 0.16; and to one O(13) sof 0.54, or O(15) sof 0.23. The lone pair is 0.27 Å from the nucleus, Fig. 2B. The coordination polyhedra for Bi(2) to Bi(5) consist essentially of severely distorted octahedra regardless of which set of disordered oxygen atoms is considered as bonding. The valence bond sums 3.13, 3.10, 3.31, and 3.39 strongly point to sole site occupancy by Bi.

The coordination polyhedron around Pb(1) is very symmetric. The cation is in the plane formed by four O(6) atoms that are 2.510(11) Å from Pb(1). The polyhedron can be completed by four O(18) atoms at 3.10(5) Å, sof 0.29, forming an elongated cube, Figs. 2B and 3, or by two O(14), sof 0.27, at 2.185(1) or by two O(20), sof 0.08, at 2.394(1), each set forming an octahedron, Fig. 2B. The calculated lone-pair location, Table 6, indicates that the $6s^2$ electrons are spherical. Pb(2) is coordinated to seven fully occupied oxygen sites and 24% of the time O(17) is present, Fig. 2B. The lone pair is 0.56 Å from the nucleus. The polyhedron formed by the eight fully occupied anion sites around Pb(3) can be considered as a distorted monocapped pentagonal bipyramid, Fig. 2B. It is the same as for Pb(2) when O(17) is present. The lone pair is 0.68 Å from the nucleus of Pb(3). The valence bond sums 2.50, 2.54, and 2.64 may indicate that Bi(1) partially occupies these three sites.

TABLE 6
Lone-Pair Positions and Distances from the Nuclei, Å

Atom	*x*	*y*	*z*	*d*
Bi(1)	0.5	0.1582	0.5	0.21
Bi(2)	0.1694	0.1329	0.1748	0.41
Bi(3)	0.3234	0.3740	0.3270	0.54
Bi(4)	0.6096	0.3041	0.9688	1.1
Bi(5)	−0.0197	0.3224	0.34	0.27
Pb(1)	0	0	0	—
Pb(2)	−0.2892	0	0.3494	0.56
Pb(3)	0.2972	0	0.3070	0.68

P(1) and P(2) atoms occupy the centers of tetrahedra. Two fairly regular tetrahedra exist around P(1): P(1)–O(9)–O(10)–2O(11) and P(1)–O(9)–O(17)–2O(16). Based on the sof of the oxygen anions the first tetrahedron is present about 76% of the time and the second 24%. The two tetrahedra have as a common apex O(9). The tetrahedra are rotated about the bond P(1)–O(9) by 55°, Fig. 1. Three somewhat less regular tetrahedra are present around P(2). The first is formed by O(12)–O(15)–2O(18), the second by O(15)–O(20)–2O(19), and the third by O(12)–O(14)–2O(13), Fig. 1. The first and second tetrahedra are related by a 55° rotation about P(2)–O(15). The third tetrahedron is obtained by a rotation of about 55° around P(2)–O(12) starting

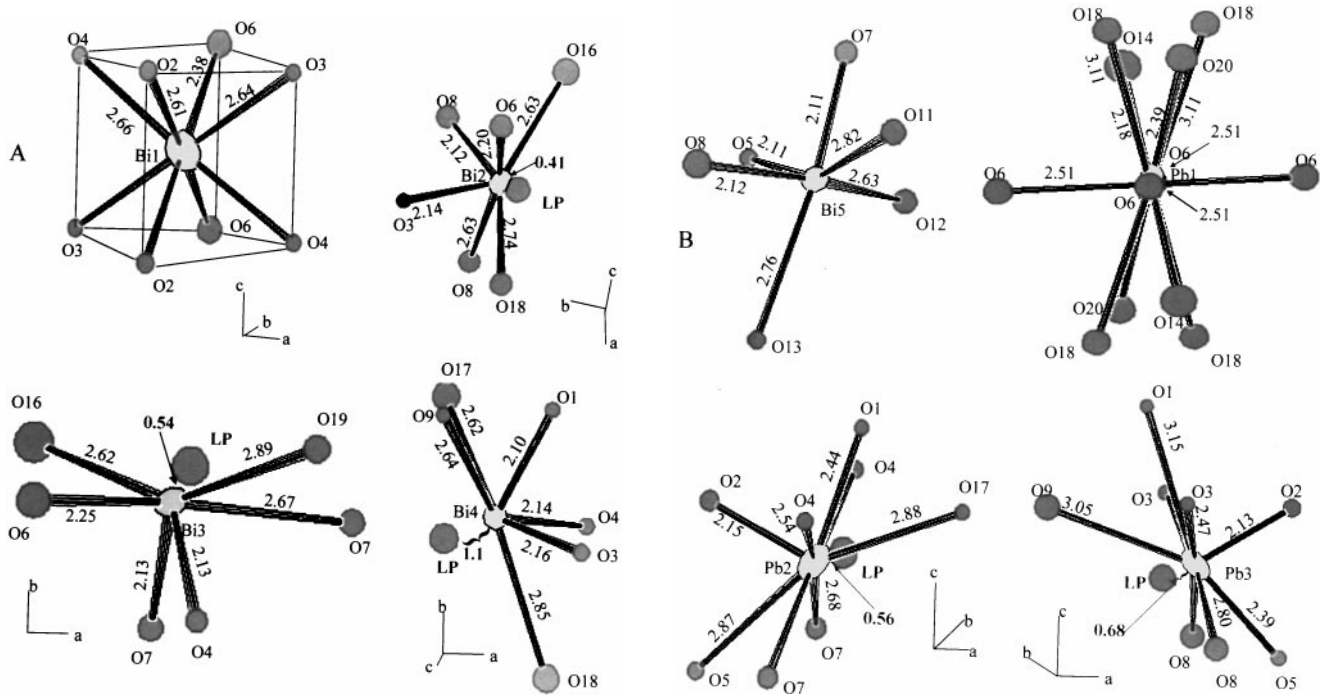

FIG. 2. Oxygen coordination polyhedra around (A) Bi(1), Bi(2), Bi(3), and Bi(4) and (B) Bi(5), Pb(1), Pb(2), and Pb(3). When equivalent bond lengths occur they are omitted. When more than one set of disordered oxygen atoms are possible only one is illustrated for the sake of clarity. However, all possible bonding oxygen atoms to Pb(1) are shown. LP represents the displacement of the lone-pair electron density from the cation nucleus.

from the first tetrahedron. All of these oxygen atoms exhibit partial occupancy as shown in Table 3. Of course, only one of each tetrahedron centered on P(1) and P(2) is present in any one unit cell and the disorder is most likely statistical creating domains within the crystal. It is not possible to fix uniquely which of the tetrahedra are simultaneously present in a given unit cell. However, based on the oxygen site occupancies the tetrahedron P(1)–O(9)–O(10)–2O(11) occurs much more frequently than P(1)–O(9)–O(18)–2O(17). Similarly the most frequently occurring tetrahedron for P(2) is P(2)–O(12)–O(14)–2O(13) and it is reasonable to assume that the most frequently occurring tetrahedra are present at the same time in a given unit cell. Selected bond lengths and angles are shown in Table 5. The interatomic distances among O(1) to O(9) are greater than 2.6 Å; bond distances among oxygen atoms with partial occupancies when they are simultaneously present range from 2.3 to 2.6 Å; unrealistically short distances, e.g., 1.5 Å, are calculated for disordered oxygen atoms that cannot simultaneously be present.

Units of Pb_2O_2 parallel to [100] result from the sharing of the polyhedral edge formed by O(2) and O(5) that are bonded to both Pb(2) and Pb(3). Two such Pb_2O_2 units bond parallel to [001] by forming a weak van der Waals bond Pb(3)–O(1), 3.147(10) Å, and a strong bond Pb(2)–O(1), 2.436(10) Å, to create Pb_4O_6 entities, Fig. 4. These tetrameric entities are separated by $P(1)O_4$ tetrahedra and by two separate $P(2)O_4$–Pb(1)–$P(2)O_4$ columns parallel to [100] that are repeated by the *c* axis periodicity, Fig. 4. This layer parallel to the *a*–*c* plane is sandwiched between

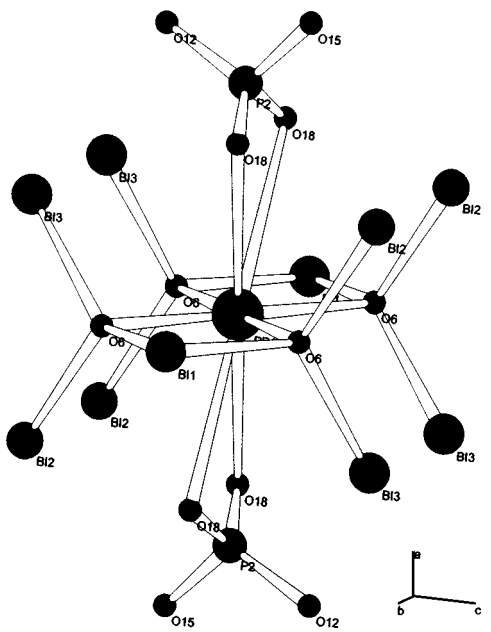

FIG. 3. Pb(1)–Bi–O articulations parallel to (010). The Pb(1)–O coordination polyhedron is an elongated cube. Only one possible orientation of $P(2)O_4$ is depicted.

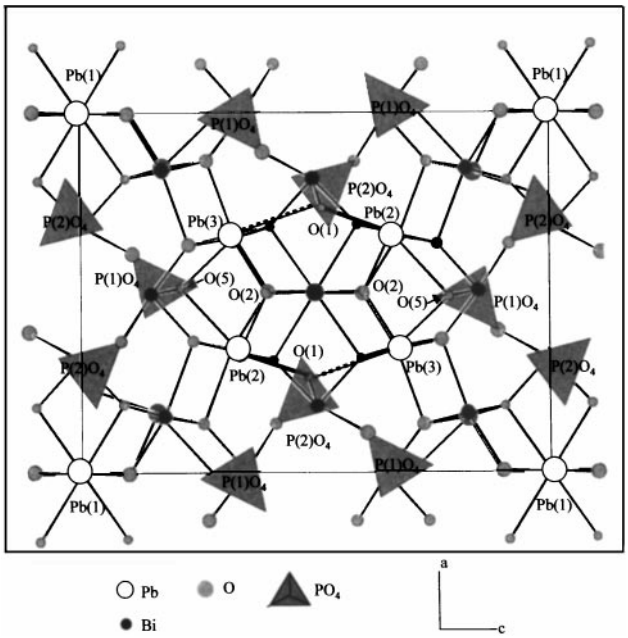

FIG. 4. Crystal structure of $Pb_5Bi_{18}P_4O_{42}$ looking along [010]. The heavy line shows the Pb(2)–O(1) 2.436(10) Å bond and the dotted line the long Pb(3)–O(1) 3.147(10) Å bond for the Pb_4O_6 moiety.

the Bi–O layers that are parallel to the *a*–*c* plane and perpendicular to [010], Fig. 3. They are interconnected along [100] by $P(2)O_4$–Pb(1)–$P(2)O_4$, Fig. 3. The two-dimensional sheets perpendicular to [010] are fused by interlayer $P(1)O_4$ groups, Pb(2), and Pb(3) into a three-dimensional network, Fig. 5.

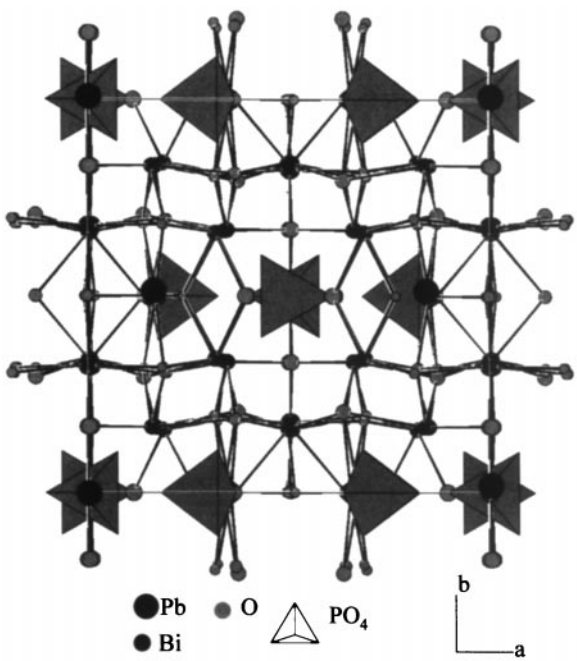

FIG. 5. Crystal structure of $Pb_5Bi_{18}P_4O_{42}$ looking along [001].

The unit cell parameters of $Pb_5Bi_{18}P_4O_{42}$ are related to those of the fluorite type δ-Bi_2O_3 by the transformation $a = \frac{3}{2}a_f - \frac{3}{2}b_f$; $b = \frac{3}{2}a_f + \frac{3}{2}b_f$; $c = 3c_f$. This corresponds approximately to a $3 \times 3 \times 3$ superstructure of a smaller tetragonal I-centered cell, $a = b = 3.9$ Å an $c = 5.5$ Å, which is based on the cubic F-centered fluorite cell $a = 5.525$ Å. The atoms Bi, Pb, and P occupy nearly the same positions as Bi in δ-Bi_2O_3. Numerous compounds adopt the same type of superstructure (14), Kashida *et al.* (11) found partial disorder of oxygen ions coordinated to V in Bi_2O_3:V_2O_5 = 9:1.

ACKNOWLEDGMENTS

S.G. and H.S. gratefully acknowledge the support of the R. A. Welch Foundation of Houston, TX. S.G. thanks the IMCCEC/US consortium under Contract No. W-31 for a travel grant. Portions of this work were performed at the DuPont–Northwestern–Dow Collaborative Access Team (DND-CAT) Synchrotron Research Center located at Sector 5 of the Advanced Photon Source. DND-CAT is supported by the E.I. DuPont de Nemours & Co., The Dow Chemical Company, the U.S. National Science Foundation through Grant DMR-9304725 and the State of Illinois through the Department of Commerce and the Board of Higher Education Grant IBHE HECA NWU 96. Use of the Advanced Photon Source was supported by the U.S. Department of Energy, Basic Energy Sciences, Office of Energy Research, under Contract No. W-31-102-Eng-38. We thank W. Marshall from DuPont and D. Keane and Z. Wawrzak from DND-CAT for their technical assistance.

REFERENCES

1. H. A. Harwig, *Z. Anorg. Allg. Chem.* **444,** 151 (1978).
2. H. A. Harwig and J. W. Weenk, *Z. Anorg. Allg. Chem.* **444,** 167 (1978).
3. L. E. Depero and L. Sangaletti, *J. Solid State Chem.* **122,** 439 (1996).
4. H. A. Harwig and A. G. Gerards, *J. Solid State Chem.* **26,** 265 (1978).
5. F. Abraham, M. F. Debreuille-Gresse, G. Mairesse, and G. Nowogrocki, *Solid State Ionics* **28–30,** 529 (1988).
6. S. Nadir and H. Steinfink, *J. Solid State Chem.* **143,** 9 (1999) and references therein.
7. J. C. Boivin and G. Mairesse, *Chem. Mater.* **10,** 2870 (1998).
8. A. M. Azad, S. Larose, and S. A. Akbar, *J. Mater. Sci.* **29,** 4135 (1994).
9. W. Zhou, *J. Solid State Chem.* **76,** 290 (1988).
10. W. Zhou, *J. Solid State Chem.* **87,** 44 (1990).
11. S. Kashida, T. Hori, and K. Nakamura, *J. Phys. Soc. Jpn.* **63** (12) 4422 (1994).
12. J. P. Wignacourt, M. Drache, P. Conflant, and J. C. Boivin, *J. Chim. Phys.* **88,** 1933 (1991).
13. J. P. Wignacourt, M. Drache, and P. Conflant, *J. Solid State Chem.* **105,** 44 (1993).
14. Y. C. Jie and W. Eysel, *Powder Diffraction* **10** (2), 76 (1995).
15. A. Mizrahi, J. P. Wignacourt, M. Drache, and P. Conflant, *J. Mater. Chem.* **5** (6), 901 (1995).
16. A. Mizrahi, J. P. Wignacourt, and H. Steinfink, *J. Solid State Chem.* **133,** 516 (1997).
17. E. P. Moore, H. Y. Chen, L. H. Brixner, and C. M. Foris, *Mater. Res Bull.* **17,** 653 (1982).
18. L. H. Brixner and C. M. Foris, *Mater. Res. Bull.* **9,** 273 (1974).

19. S. Giraud, J. P. Wignacourt, M. Drache, G. Nowogrocki, and H. Steinfink, *J. Solid State Chem.* **142,** 80 (1999).
20. S. Giraud, P. Conflant, M. Drache, J. P. Wignacourt, and H. Steinfink, *J. Inorg. Phosphorus Chem. Phosphorus Res. Bull.* **10,** 138 (1999).
21. Z. Otwinowski and W. Minor, *Methods Enzymol.* **276,** 307 (1997).
22. G. Sheldrick, SHELXS-86, Institut für Anorganische Chemie, Gottingen, 1985.
23. G. Sheldrick, SHELXL-93, Institut für Anorganische Chemie, Gottingen, 1993.
24. D. Brown and D. Altermatt, *Acta Crystallogr. B* **41,** 244 (1985).
25. J. Galy and R. Enjalbert, *J. Solid State Chem.* **44,** 1 (1982).
26. N. Jakubowicz, O. Perez, D. Grebille, and H. Leligny, *J. Solid State Chem.* **139,** 194 (1998).
27. L. Shimoni-Livny, J. P. Glusker, and C. W. Bock, *Inorg. Chem.* **37,** 1853 (1998).
28. A. Verbaere, R. Marchand, and M. Tournoux, *J. Solid State Chem.* **23,** 383 (1978).
29. P. P. Ewald, *Ann. Phys.* **64,** 253 (1921).
30. D. Le Bellac, J. M. Kiat, and P. Garnier, *J. Solid State Chem.* **114,** 459 (1995).
31. E. Morin, G. Wallez, S. Jaulmes, J. C. Couturier, and M. Quarton, *J. Solid State Chem.* **137,** 283 (1998).